[33] M. Diaz Peña and G. Tardajos, J. Chem. Thermodyn. *11*, 441 (1979).
[34] R. C. Wilhoit and B. J. Zwolinski, Physical and Thermodynamic Properties of Aliphatic Alcohols, J. Phys. Chem. Ref. Data (NBS) Vol. 2, 1 (1973).
[35] Landolt-Börnstein, Zahlenwerte und Funktionen, Vol. II, 1, Springer, Berlin 1971.
[36] N. B. Vargaftik, Tables on Thermodynamical Properties of Liquids and Gases, J. Wiley, New York 1975.
[37] A. J. Treszczanowicz and G. C. Benson, J. Chem. Thermodyn. *9*, 1189 (1977), ibid. *10*, 967 (1978), ibid. *12*, 173 (1980).
[38] A. J. Treszczanowicz, O. Kiyohara, and G. C. Benson, J. Chem. Thermodyn. *13*, 253 (1981).
[39] D. Eßwein, A. Heintz, B. Schmittecker, and R. N. Lichtenthaler, J. Chem. Thermodyn., in press.
[40] P. Jeschke and G. M. Schneider, J. Chem. Thermodyn. *10*, 803 (1978).
[41] A. Bondi, Physical Properties of Molecular Crystals, Liquids and Glases, J. Wiley, New York 1968.
[42] G. Geiseler and H. Seidel, Die Wasserstoffbrückenbindung, Akademie Verlag, Berlin 1977.
[43] L. Saroléa-Mathot, Trans. Faraday Soc. *49*, 8 (1953).

(Eingegangen am 21. August 1984, endgültige Fassung am 10. November 1984) E 5819

High Temperature Reaction Rate for H + O_2 = OH + O and OH + H_2 = H_2O + H

P. Frank and Th. Just

DFVLR, Institut für Physikalische Chemie der Verbrennung, Stuttgart, West-Germany

Chemical Kinetics / Elementary Reactions / Shock Waves

Shock heating together with atomic resonance absorption spectrometry (ARAS) was used to record simultaneously H- and O-atom concentration profiles in the post-shock region behind reflected shocks. The dissociation of N_2O together with the reaction O + H_2 = OH + H was used as a source of H and OH for the reactions H + O_2 = OH + O and OH + H_2 = H_2O + H. The test gas mixtures consisted of argon with relative concentrations of a few ppm N_2O and 100 to 500 ppm H_2 and O_2. The experiments were conducted in the temperature range of 1700 to 2500 K at total densities of $6 \cdot 10^{-6}$ to $1.3 \cdot 10^{-5}$ mol cm^{-3}. The following rate coefficients were deduced:

R1 H + O_2 = OH + O
$k_1 = (2.44 \pm 0.33) \cdot 10^{14}$ cm^3 mol^{-1} s^{-1} exp − [(72.3 ± 2.2) kJ mol^{-1}/RT]

R2 OH + H_2 = H_2O + H
$k_2 = (4.74 \pm 0.65) \cdot 10^{13}$ cm^3 mol^{-1} s^{-1} exp − [(25.5 ± 2.2) kJ mol^{-1}/RT].

For temperatures below 2500 K nearly complete agreement with the value for the rate coefficient of reaction R1 as recommended by Baulch [1] was obtained. For reaction R2 a rate coefficient was deduced which is close to the value as given by Gardiner et al. [23].

Introduction

Hydrogen-oxygen reactions play a prominent role as part of the main chain-branching processes in the high-temperature combustion of hydrocarbons. It is well established that only a few reactions including R1, R2 are relevant for describing the ignition mechanism under flame conditions [3]. The most important rate controlling elementary step under most conditions is the reaction of H-atoms with molecular oxygen. In typical hydrocarbon-air-flames at pressures around 1 bar, O_2 is mainly consumed by reaction R1. A study of the extensive literature and comprehensive reviews on hydrogen-oxygen reactions [1, 4, 5] reveals a considerable scatter in the data for the high-temperature rate coefficient of H + O_2 = OH + O. Due to the well known high sensitivity of many reaction systems under flame or shock tube conditions on this reaction (see e.g. Ref. [5 – 7]), a more precise determination of the rate coefficient of this elementary step seems desirable.

The aim of the present study is to measure the rate of the reaction

R1 H + O_2 = OH + O

in a highly diluted system, so that the effect of subsequent reactions can be reduced considerably. The H-atoms were produced by the reaction of O-atoms with molecular hydrogen

R3 O + H_2 = OH + H.

O-atoms were delivered by the thermal dissociation of small amounts of N_2O

R4 N_2O + Ar = N_2 + O + Ar.

The rate coefficient for this reaction is well established in the pressure range of the present experiments [8 – 10]. The authors made recently a reinvestigation of this important reaction by applying two different methods of measurement. The results will be presented below.

It is to be expected [5] that the chain propagating reaction

R2 OH + H_2 = H_2O + H

will also have influence on the radical production in the system under investigation.

Experimental

Details of the shock tube as well as the optical setup have been described elsewhere [9, 11] and only a short summary will be presented below:

The brass shock tube consists of a test section of about 7 m in length and a driver section of 4 m. The internal diameter is 7.5 cm. The test section is evacuated by a turbomolecular pump to less than 10^{-7} mbar before each experiment. Mixtures are prepared and stored in a stirred 56-l stainless steel vessel which is bakeable up to 250°C. The measurements were performed behind the reflected shock front close to the end flange (5 mm). Atomic resonance absorption (ARAS) was used to monitor time-dependent H- and O-atom concentrations. As light sources for the absorption measurements, microwave-excited discharge lamps which contain O_2 or H_2 diluted in He, were used.

H- and O-concentrations can be measured simultaneously by using an oxygen spectral filter (for H-atoms at 121.5 nm) and a 1 m vuv-monochromator for O-atoms (at 130.5 nm). The spectral filter [9, 12] is combined with a solarblind photomultiplier and a L_α-interference filter of 15 nm HBW. This filter was used to reduce lamp radiation originating from H_2-emission in the wavelength region around 160 nm. The transmitted intensity signals were recorded by a 2-channel transient recorder with 2 kB per channel and transferred to a HP 87 personal computer. A program computes an averaged signal and transfers the intensity via calibration curves into particle density versus time plots.

Because of the high sensitivity of the optical measurement technique ($[H] > 5 \cdot 10^{11}$ cm^{-3}; $[O] > 10^{12}$ cm^{-3}) very small initial concentrations of the reactants could be used. All gases were of ultrahigh purity: H_2 > 99.9997%, O_2 > 99.998%, N_2O > 99.99%, Ar > 99.9999%. The range of the test gas mixtures used is given in Table I.

Table I
Range of test gas mixtures in argon (in ppm)

Mixture:	A	B	C	D	E
N_2O	5	5	2.5	2	2
H_2	500	250	125	200	100
O_2	500	512	256	200	200

Evaluation

1. Temperature

The speed of the incident shock near the end flange was obtained by linear extrapolation of the measured speeds between the four thin-film gauges. The temperature behind the reflected shock near the end flange was calculated by solving the appropriate conservation equations. It was assumed that the temperature so calculated agrees with the real gas temperature occuring immediately behind the reflected shock.

This assumption is supported by careful direct temperature measurements in this shock tube several years ago behind incident shocks [22]. In these experiments absolute temperatures by Na-line and CO_2-band emission-absorption methods were determined. The used black-body radiator (graphite) gave radiation temperatures which agreed within less than 5° with thermocouple measurements within the graphite radiator and with measurements using a calibrated pyrometer. The direct measurements immediately behind the incident shocks agreed with the calculated ones from the measured local shock speed within ± 1.5%. In most cases the agreement was even better.

Using the following error factors

i) shock speed determination	± 0.2%
ii) measurement of absorption signal	± 5%
iii) time scale determination	± 10 µsec
iv) rate coefficient for N_2O-decay	± 20%

and a typical first order reaction such as N_2O-decay, we arrive at an uncertainty factor of ± 1% in the temperature of the reflected shock. This is in good agreement with the above mentioned results for the incident shock. The so calculated temperature is valid only for gas zones immediately behind the shock front. At long distances the temperature changes slightly. Experiments with CO_2-mixtures served as control experiments for the constancy of the temperature behind the reflected shock. At 4.41 µm the intensity profiles for optical thin conditions with time were monitored [15]. They revealed small deviations from the assumption of constant temperature in the post shock region behind reflected shocks. From these experiments, assuming adiabatic changes, an average temperature drop, linear in time, of 2% at 400 µsec for total pressures around 2 bar has been derived. Temperature corrections are taken into account in all experiments including calibration experiments in which initiation reactions with relatively large activation energies like the N_2O decay are involved. For temperatures around 1700 K the O-atom formation from N_2O is very slow and therefore sensitive to slight temperature alterations, whereas at temperatures above 1950 K the temperature corrections are negligible with respect to the reaction system under investigation.

2. Calibration of H- and O-Concentrations

The H- and O-concentration profiles reported here are based on calibration measurements. The necessary H-atoms for calibration at $T > 2100$ K are produced through the well known hydrogen dissociation reaction R10 (Table II). The value for k_{10}, as recommended by Baulch et al. [1], deviates in the temperature range between 2100 and 2500 K from that given by Myerson and Watt [13], who monitored the H-atom concentration via ARAS, only by less than 5%. Hence, either of the expressions can be used. Because of the slow thermal decay of H_2 at temperatures below 2000 K, the calibration in the low temperature range of 1600 to 2100 K is performed by using the reaction of O-atoms (from the N_2O-dissociation) with H_2 [14].

Table II
Reaction mechanism and rate coefficient expressions

	Reaction	A	n	E_a	Ref.
R1	$H + O_2 = OH + O$	$2.44 \cdot 10^{14}$	0.0	72.3	×
R2	$OH + H_2 = H_2O + H$	$4.74 \cdot 10^{13}$	0.0	25.5	×
R3	$O + H_2 = OH + H$	$1.85 \cdot 10^{14}$	0.0	58.0	×
R4	$N_2O + Ar = N_2 + O + Ar$	$9.30 \cdot 10^{14}$	0.0	248.8	×
R5	$N_2O + O = NO + NO$	$1.00 \cdot 10^{14}$	0.0	117.2	[1]
R6	$N_2O + H = OH + N_2$	$7.60 \cdot 10^{13}$	0.0	63.0	[1]
R7	$H_2O + O = OH + OH$	$1.50 \cdot 10^{10}$	1.14	72.0	[5]
R8	$O_2 + Ar = O + O + Ar$	$1.80 \cdot 10^{18}$	−1.0	494.0	[1]
R9	$H_2 + O_2 = OH + OH$	$1.70 \cdot 10^{13}$	0.0	201.0	[18]
R10	$H_2 + Ar = H + H + Ar$	$2.20 \cdot 10^{14}$	0.0	402.0	[1]
				×: this work	

Rate coefficients are expressed in the form $k = A \cdot T^n \cdot \exp(-E_a/RT)$. Units are cm^3 mol^{-1} s^{-1} and kJ.

The dissociation reaction of N_2O served also for obtaining O-atom calibration curves. At temperatures above 2200 K, partial equilibrium $[O] = [N_2O]_0$ is achieved within the observation time. Above this temperature the evaluation of the O-atom calibration curves is free from errors caused possibly by the kinetics of the N_2O-dissociation.

The background absorption of N_2O and H_2 at both wavelengths was taken into account if necessary. The temperature dependent absorption of O_2 [17] at 121.5 nm was in all experiments less than 3%, yet it was considered. The used cross-sections for absorption were:

$\sigma(N_2O) = 6 \cdot 10^{-18}$: ($L_\alpha$); and $5.5 \cdot 10^{-17}$: (O-triplet)

$\sigma(H_2) = 4.2 \cdot 10^{-17} \exp(-9986/T)$: ($L_\alpha$)*; and ≈ 0: (O-triplet)

$\sigma(O_2) = 7.1 \cdot 10^{-22} \cdot T - 6.3 \cdot 10^{-19}$: ($L_\alpha$); and $5 \cdot 10^{-19}$: (O-triplet)

(All cross-sections are in cm^2; *: Ref. [15]).

Data interpretation was performed with the aid of computer modeling. The rate coefficient for the reverse reaction was always computed from the forward rate coefficient and the equilibrium constant K_c. Thermochemical properties for calculating K_c were computed from polynomial fits to JANAF.

Results

N_2O-Decomposition:

Since the N_2O-decomposition plays an important role in our experiments, the dissociation reaction of N_2O in argon has been reinvesti-

gated. Relative N_2O concentrations in the range from 0.25 to 500 ppm were applied.

At this point it should be mentioned that fortunately N_2O as well as O_2 and H_2, show practically no wall adsorption when mixtures are prepared and filled into the shock tube. Fig. 1 shows the excellent agreement between N_2O mixtures, which differed in the initial concentrations by factors up to 500 but gave nearly identical results at closely neighbouring temperatures. The error in the N_2O concentration is given by the error of the pressure gauge and the applied multistep mixing procedure. This error never exceeded ± 5% for the N_2O concentration. That is marginal, considering the experimental scatter given by temperature uncertainties in calibration experiments with slow dissociation rates.

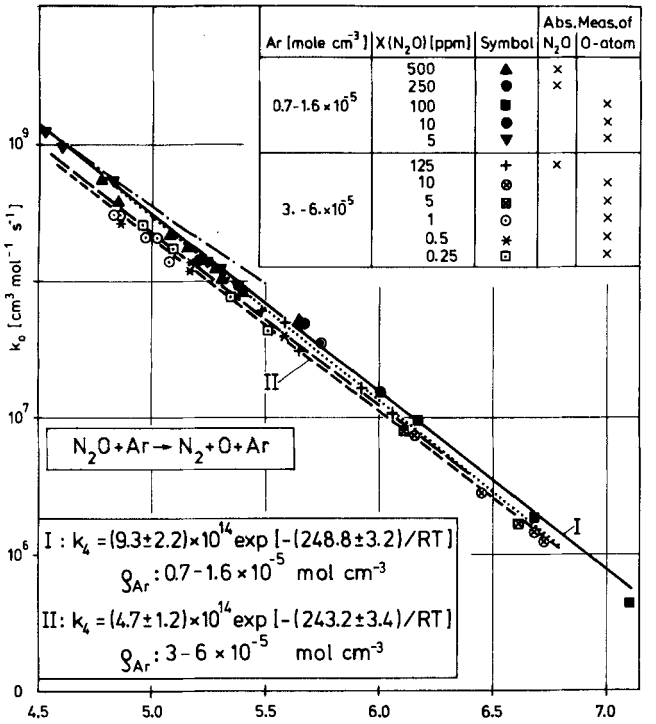

Fig. 1
Arrhenius diagram of evaluated values for the rate coefficients of $N_2O + Ar = N_2 + O + Ar$.
Full line: this work, [Ar] = $0.7 - 1.6 \cdot 10^{-5}$ mol cm^{-3}
----------: this work, [Ar] = $3.0 - 6.0 \cdot 10^{-5}$
.....: Ref. [8] [Ar] < $1.4 \cdot 10^{-5}$
– – –: Ref. [10] [Ar] < $6.0 \cdot 10^{-5}$
– · – · –: Ref. [21] [Ar] < $3.0 \cdot 10^{-6}$

The temperature ranged from 1450 to 2220 K. Two different methods were used:

For the total density range of $0.7 - 1.6 \cdot 10^{-5}$ mol cm^{-3} with very small initial concentrations of N_2O (5 – 100 ppm), the rate of reaction was measured by monitoring the time-dependent O-atom concentration by ARAS.

The decrease of the N_2O-concentration in the same density range has been measured by monitoring the absorption of N_2O at 1282 Å. As the absorption of N_2O follows sufficiently good the Lambert-Beer-law, and the absorption coefficient of N_2O ($\approx 6 \cdot 10^{-17}$ cm^2) at 1900 K) exceeds by more than a factor 30 the absorption cross-sections of N_2 and NO, the evaluation of k_4 could be performed by experiments, which were self-calibrating. Even for the highest values of the initial concentration ($X(N_2O)$ = 500 ppm), it was found that the reaction mechanism of the N_2O-dissociation can be described by reaction R4 and the subsequent reaction R5, $N_2O + O = NO + NO$ (or $N_2 + O_2$), which fortunately under our conditions has a minor influence on the evaluation of k_4.

Fig. 1 shows an Arrhenius plot of k_4 as second order rate constant for two different density ranges. The plot shows that especially for the lower pressure range (full symbols in Fig. 1) – which corresponds to the range of the $N_2O/H_2/O_2$-experiments – there is very good agreement between O-atom-ARAS and N_2O-absorption measurements. The derived expression for k_4 agrees very well with the expression given by Roth and Just [8] for temperatures above 1900 K, and is about 25% higher at 1500 K. The rate expression of Monat et al. [21] shows good agreement around 2000 K, whereas recent measurements of Louge and Hanson [25] are in good correspondence with our results between 1700 and 2000 K. The values reported by Olschewsky et al. [10] are slightly smaller at the lower pressures and fit the set of data for the higher pressure range very well. For this pressure range, the second order rate coefficients are about 30% smaller at 2000 K than for the lower pressure range, which may indicate, that the reaction proceeds already in the fall-off regime. This is in good agreement with the finding in Ref. [10] that the low pressure regime for N_2O-dissociation "ends" at about $6 \cdot 10^{-5}$ mol cm^{-3}.

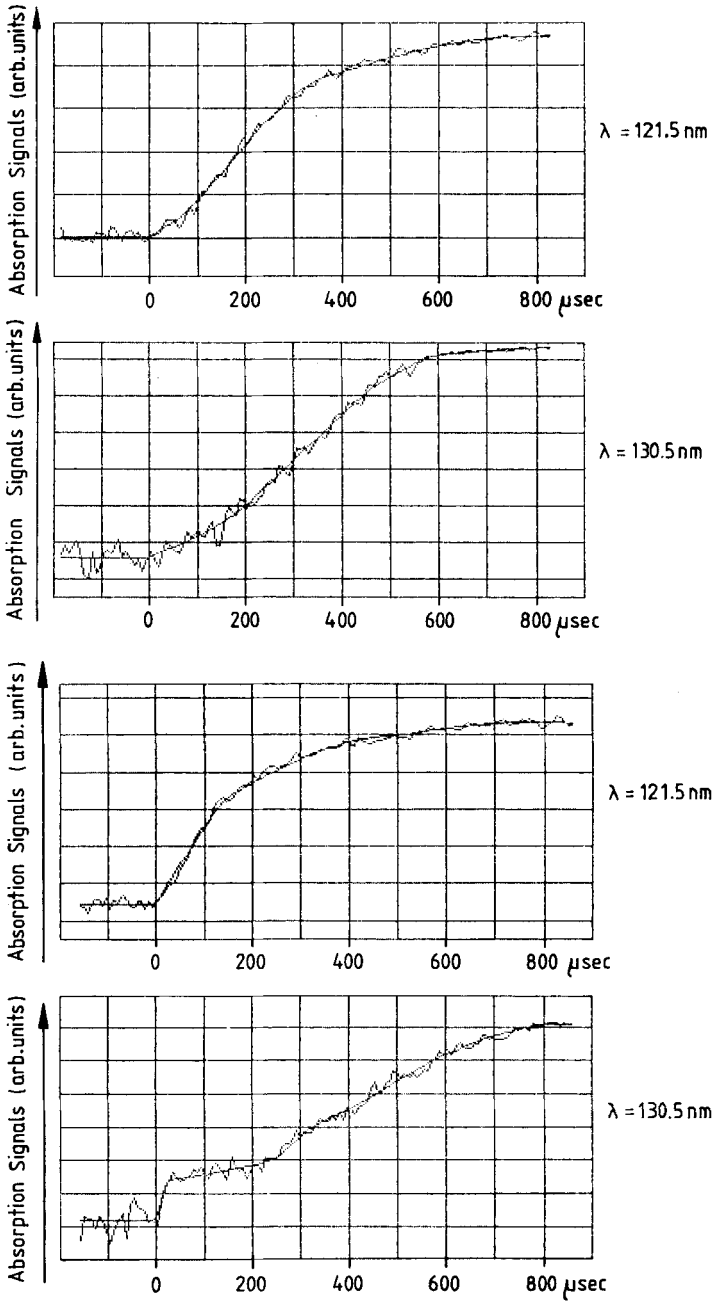

Fig. 2
Typical absorption signals of H- (upper print-out) and O-atoms (lower print-out).
a: mixture B, T = 1838 K
b: mixture E, T = 2430 K

$N_2O - H_2 - O_2$ Reactions:

Fig. 2 shows typical absorption profiles of H- and O-atoms under two different conditions. The smoothed curve in each plot represents the averaged signal as calculated by the computer program. Point $t = 0$ μsec at the abscissa, the onset of the reaction, is calculated from the shock front speed, extrapolated to the observation station. In the cases where a steep signal increase immediately after the reflected shock front was observed, the calculated onset agreed always within ± 10 μsec with the observed one. At lower temperatures (Fig. 2a, lower half) the O-atom production is slow, due to the small thermal dissociation of N_2O. With increasing time H-atoms, which are produced via the reaction of O-atoms with H_2, can now react with O_2. Hence, the rates of O-atom as well as H-atom production are increased by chain-branching. At high temperatures (Fig. 2b, lower half) O-atoms are formed nearly instantaneously in the post-shock region, which can clearly be seen by the step in the O-absorption profile. In the following 200 μsec most of the additionally produced O-atoms are consumed by the reaction with H_2. This increases the H-atom concentration considerably. After this induction period for the O-atoms, the O-atom concentration increases mainly by the chain-branching reaction of O_2 with H-atoms.

A ten-step reaction mechanism was adopted for calculating the particle density profiles as given in Table II.

For displaying the sensitivity of the computed H- and O-atom concentrations, a low and a high temperature (1693 and 2389 K) experiment with a mixing ratio of $N_2O:H_2:O_2$ = 1:50:100 was selected (Fig. 3). At the chosen reaction time of 600 μsec, the chain-branching and -propagating mechanism is completely switched on. The sensitivities of the particle density profiles on the rate coefficients k_1 to k_4 are considerable under these conditions.

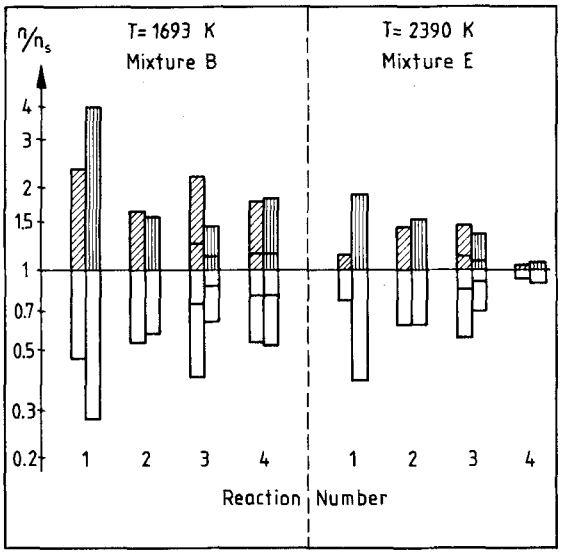

Fig. 3
Sensitivity of H- and O-concentration for $N_2O:H_2:O_2$ = 1:50:100 mixtures. n/ns represents changes in H (left box) – and O (right box) – concentrations at 600 μsec by multiplying the rate expressions of Table II by 2 (dashed boxes) and 0.5 (open boxes). All noticeable changes are included. Bars in the boxes for reactions R3 and R4 correspond to changes of k_3 and k_4 by ± 20%

The sensitivity analysis shows that besides the reactions of interest R1 and R2, in particular, reactions R3 and R4 have considerable influence on the profiles. The first step was therefore, to fix reliable limits for the rate coefficients for these two reactions:

The dissociation of N_2O is well investigated for the range of our experimental conditions [8, 10] and our own measurements for the density range of these experiments of both, the O-atom production and the N_2O-decay, gave a value for the rate coefficient which is very close to the data of Roth and Just [8], as discussed above. From these results we estimate the scatter in the rate coefficient for R4 to be less than ± 20%.

Reaction R3 has been investigated extensively by numerous authors [1, 15, 19, 24]. In a recent study, Pamidimukkala and Skinner [19] measured O-atom profiles of $N_2O - H_2 - Ar$ mixtures in the post-shock region and deduced a value for k_3 which is very close to that of Schott et al. [24]. We have also performed such experiments with simultaneous measurements of H- and O-profiles (Figs. 4 and 5). A sensitivity analysis demonstrates that only reaction R3 and R4 influence the particle density profiles remarkably (Fig. 6). Concentration profiles have been calculated by varying k_3 between the value given in Ref. [19] and a value close to that recommended by Baulch et al. [1]. The best fit was achieved if we reduce the value of Pamidimukkala and Skinner by 20% (Fig. 4 and 5). For comparison we have also computed the profiles if the N_2O-decay is changed by 20%, which corresponds to the scatter of our measurements for k_4. This results around 1850 K only in a moderate change in the concentration of the O-atoms. We conclude from our experiments that the value of the pre-exponential factor for the rate coefficient of R3 should be slightly smaller (about 10 to 20%) than given in Ref. [19]. We used this slightly reduced rate coefficient for the evaluation of the $N_2O/H_2/O_2$-experiments. With the limits of scatter fixed for the rate coefficients of reactions R3 and R4 to ± 20%,

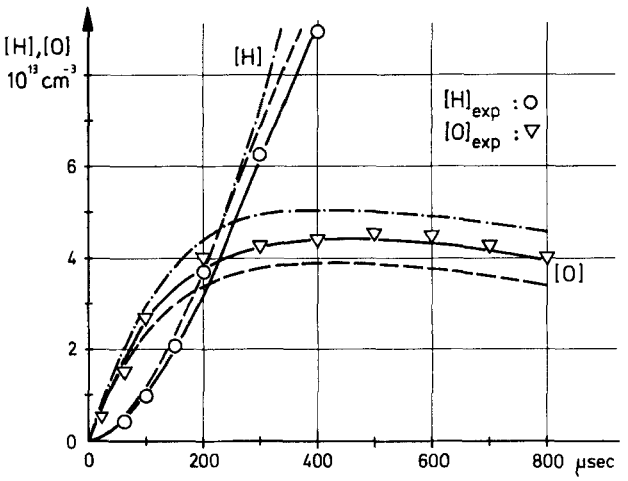

Fig. 4
Comparison between experimental results of H- and O-atom measurements and computational results.
N20: 50 ppm, H_2: 100 ppm, T = 1845 K, p = 1.75 bar
Full line: calculated with the k-values of Table II
– – – –: calc. with k_3 (Ref. [19])
– · – · –: calc. with $k_4 \cdot 1.2$

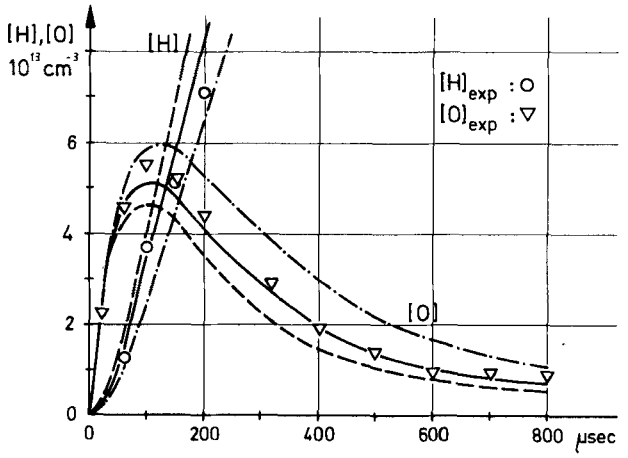

Fig. 5
Comparison between experimental results of H- and O-atom measurements and computational results.
N20: 20 ppm, H_2: 100 ppm, T = 2240 K, p = 1.64 bar
Full line: calculated with the k-values of Table II
– – – –: calc. with k_3 (Ref. [19])
– · – · –: calc. with k_3 (Ref. [1])

the sensitivity analysis (Fig. 3, bars in the boxes for R3 and R4) shows that the change in the H- and especially O-profiles depends mainly on the value of k_1.

Fig. 7 shows measured H- and O-atom concentrations for a typical low temperature experiment. Due to the small amount of O-atoms in the earlier stages of the reaction, the increase in the production of both species H and O, is only moderate within the observation time. The best fit in this example is achieved with a k_1 from Table II times 0.9. For comparison calculated profiles are shown, if a value for the reaction R1 is used as given by Schott [2]. This corresponds at this temperature to k_1 (Schott) = $k_1 \cdot 0.65$. If the value for reaction R2 is increased by a factor of 3 in order to fit the measured O-atom profile again, the calculated H-atom concentrations are then definitely much too large with respect to the measured ones.

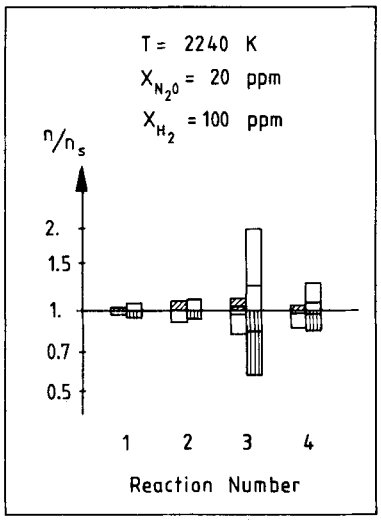

Fig. 6
Sensitivity of H- and O-profiles at 2240 K for N_2O/H_2-mixtures. n/ns represents changes in H (left box) – and O (right box) – concentrations at 400 μsec by multiplying the rate expressions of Table II by 2 (dashed boxes) and 0.5 (open boxes). All noticeable changes are included. Bars in the boxes for reactions R3 and R4 correspond to changes of k_3 and k_4 by ± 20%

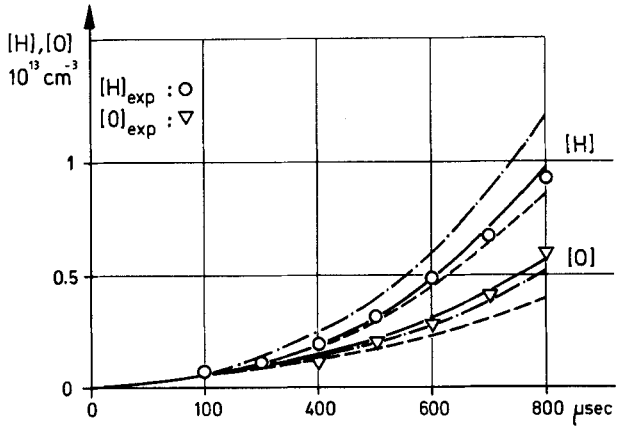

Fig. 7
Comparison between H- and O-atom measurements in $N_2O/H_2/O_2$-mixtures and computational results obtained by different sets of rate coefficients.
Mixture: C, T = 1710 K, p = 1.74 bar
Full line: calculated with $k_1 \cdot 0.9$
– – – –: calc. with k_1 (Ref. [2])
– · – · –: calc. with k_1 (Ref. [2]), $k_2 \cdot 3$

At temperatures above 2000 K there is a pronounced acceleration of the O-atom production during the second part of the observation period. For the presented experiment (Fig. 8) the best fit is achieved if one of the rate coefficients for R2 or R3 is slightly increased (factor 1.2 – 1.3). These variations in the rate coefficients lay all within the range of the experimental scatter. If the value for k_1 of Ref. [2] is used again for the reaction R1: $k_1 \cdot 0.5$, a very pronounced deviation from the measured O-atom profiles is observed.

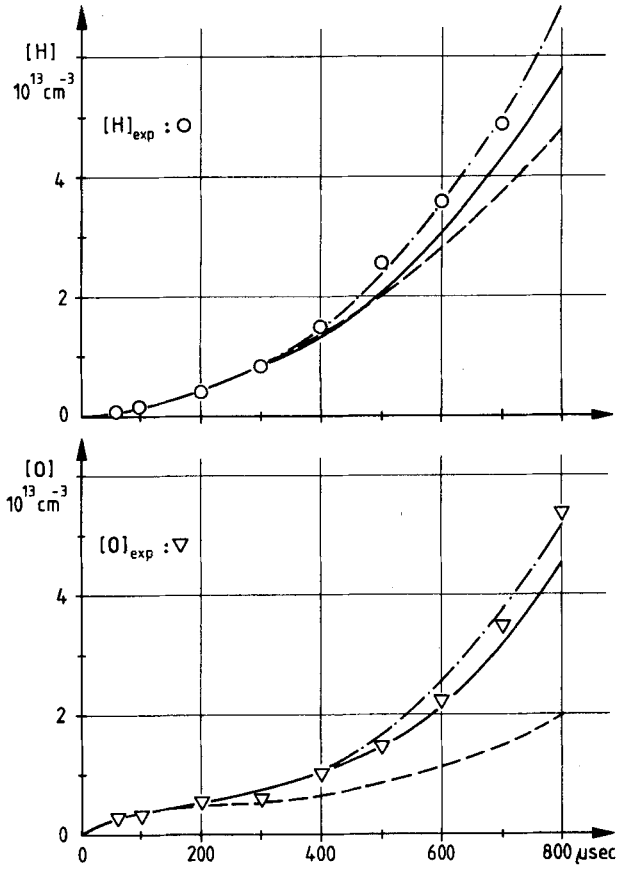

Fig. 8
Comparison between H- and O-atom measurements in $N_2O/H_2/O_2$-mixtures and computational results obtained by different sets of rate coefficients.
Mixture: E, T = 2070 K, p = 1.60 bar
Full line: calculated with the k-values of Table II
– – – –: calc. with k_1 (Ref. [2]), $k_2 \cdot 1.3$
– · – · –: calc. with $k_2 \cdot 1.3$ or $k_3 \cdot 1.2$

The same behaviour is also shown in Fig. 9. Here, at a temperature near 2400 K, the O-atoms are produced nearly instantaneously by the N_2O-decay. After an induction period, the O-atom concentration increases rapidly. Using the value for k_1 as given in Ref. [2], k_1 (Schott) = $k_1 \cdot 0.5$, the calculated profiles show very low O-atom concentrations and also smaller H-atom concentrations in the later stages of the observation time. For $k_2 \cdot 5$, an O-atom concentration is calculated, which is still too small, whereas the H-atom concentrations already exceed the measured values considerably.

Discussion

The kinetic behaviour of the system can be represented – under the present experimental conditions – by a reaction scheme, whose major features can be described by just four elementary reactions. Two of them, the N_2O-decay R4 and the reaction of H_2 with atomic oxygen R3, have been investigated separately by different authors and by us. The scatter of the rate coefficients are within ± 20% including the recent N_2O-results of Louge and Hanson [25] at lower temperatures and the values for k_3 of Ref. [19]. The influence of these inaccuracies

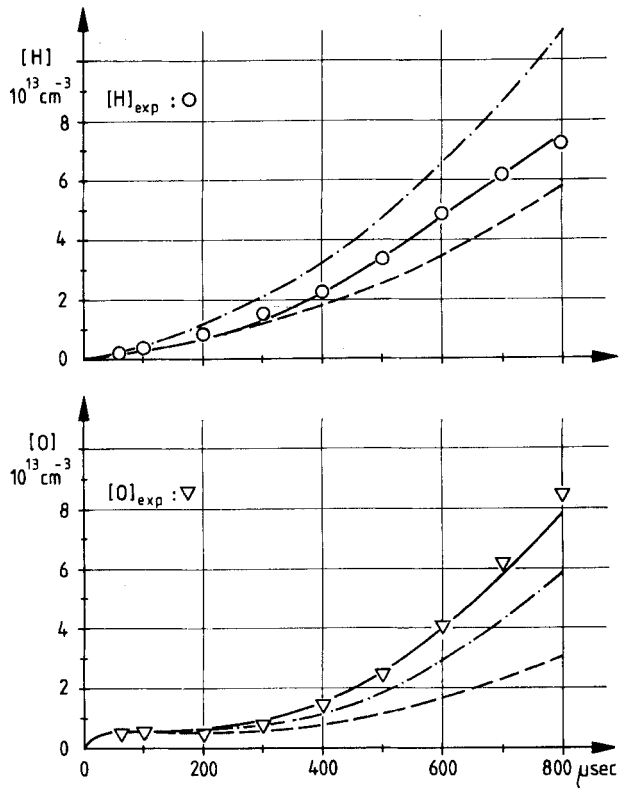

Fig. 9
Comparison between H- and O-atom measurements in $N_2O/H_2/O_2$-mixtures and computational results obtained by different sets of rate coefficients.
Mixture: E, T = 2368 K, p = 1.42 bar
Full line: calculated with the k-values of Table II
– – – –: calc. with k_1 (Ref. [2])
– · – · –: calc. with k_1 (Ref. [2]), $k_2 \cdot 5$

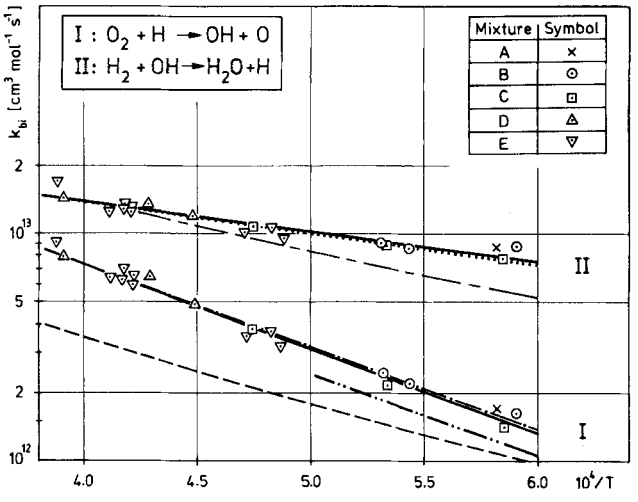

Fig. 10
Arrhenius diagram of evaluated values for the rate coefficients of H + O_2 = OH + O (curve I) and OH + H_2 = H_2O + H (curve II).
Full line: this work ……: Ref. [23] (extrapolated)
– · – · –: Ref. [1] – – – –: Ref. [2]
– · · – · ·: Ref. [26] – – – – –: Ref. [5]

(± 20%) in k_3 and k_4 on the evaluation of k_1 is in all experiments equal or less than these scatter limits.

The sensitivity analysis shows, that the dependence of the rate of reaction R1 on the value for the rate coefficient of reaction R2 should be moderate in highly diluted mixtures. As the value of k_1 is much more sensitive with respect to the O-atom concentration than to the H-atoms (see Fig. 3), whereas reaction R2 influences the concentration of both species in the same order, we can clearly deduce k_1 from the O-atom profiles. For k_2 it is difficult from the present experiments to evaluate a very accurate Arrhenius expression, because this evaluation has to be based mainly on the measurement of H-atom concentrations in the later stages of the observation period. Under the chosen experimental conditions the measured H-atom concentrations between 600 and 800 µsec are near the upper limit of the validity range of our calibration curve, which results in a reduced accuracy.

The Arrhenius plot, as given in Fig. 10 (curve I) for k_1 gives an analytical expression, which is nearly identical with the value given in the Baulch collection [1]. It differs from the values of Ref. [2] by more than a factor 1.8 at temperatures above 2000 K and even at temperatures around 1700 K, there exists a deviation of about 50%. Two experimental studies [26, 27] at temperatures below 2000 K give values for k_1 which are smaller by 30% and more compared to our results.

Our experimental findings, that there is no noticeable "negative" curvature ($\sim T^{-0.91}$) of the Arrhenius curve for reaction R1 in the temperature range between 1600 and 2500 K agree well with a recent theoretical work on k_1 [20].

For reaction R2 from the Arrhenius plot (Fig. 10, curve II) an expression is deduced, which is close to that of Gardiner et al. [23], but it should be pointed out, that the sensitivity of the measured profiles, with respect to the value of k_2, is not as good as in the case of R1. We estimate from our modeling of the experimental profiles a scatter of less than ± 40% in the evaluation of k_2. This corresponds fairly well to the observed scatter of our evaluated data points (Fig. 10).

The authors wish to thank Mrs. B. Rudo for her assistance in the performance of the experiments. The financial support of the Deutsche Forschungsgemeinschaft is gratefully acknowledged.

References

[1] D. L. Baulch, D. D. Drysdale, D. G. Horne, and A. C. Lloyd, Evaluated Kinetic Data for High Temperature Reactions, Vol. 1 (Butterworths, London 1972).
[2] G. L. Schott, Combust. Flame *21*, 357 (1973).
[3] J. Warnatz, Combust. Sci. Technol. *26*, 203 (1981).
[4] G. Dixon-Lewis and D. J. Williams, in Comprehensive Chemical Kinetics, Vol. 17, edited by C. H. Bamford and C. F. H. Tipper, (Elsevier, Oxford 1977).
[5] J. Warnatz, Survey of Rate Coefficients in C/H/O-Systems, Sandia-Report, SAND 83-8606 (1983).
[6] Y. Hidaka, C. S. Eubank, W. C. Gardiner, Jr., and S. M. Hwang, J. Phys. Chem. *88*, 1006 (1984).
[7] P. Roth and Th. Just, Symp. (Int.) on Combustion *20*, 1984, to be published.
[8] P. Roth and Th. Just, Ber. Bunsenges. Phys. Chem. *81*, 572 (1977).
[9] Th. Just, ARAS in Shock Tubes. In A. Lifshitz: Shock Waves in Chemistry, Marcel Decker, New York 1981.
[10] H. A. Olschewski, J. Troe, and H. Gg. Wagner, Ber. Bunsenges. Phys. Chem. *70*, 450 (1966).
[11] Th. Just, P. Roth, and R. Damm, Symp. (Int.) on Combustion *16*, 961 (1977).
[12] D. Appel and J. P. Appleton, Symp. (Int.) on Combustion *15*, 701 (1975).
[13] A. L. Myerson and W. S. Watt, J. Chem. Phys. *49*, 425 (1968).

[14] P. Frank and Th. Just, Combust. Flame *38*, 231 (1980).
[15] G. Rimpel, DFVLR Inst. f. Phys. Chem. d. Verbrennung, Stuttgart, unpublished work.
[16] Th. Just, Proceedings 13th Int. Symp. on Shock Tubes and Waves, 54, State University of New York Press, Albany 1982.
[17] K. A. Bhaskaran, P. Frank, and Th. Just, Proceedings 12th Int. Symp. on Shock Tubes and Waves, 503, The Magnus Press, Jerusalem 1980.
[18] C. J. Jachimowski and W. M. Houghton, Combust. Flame *17*, 25 (1971).
[19] K. M. Pamidimukkala and G. B. Skinner, J. Chem. Phys. *76*, 311 (1982).
[20] J. Troe, Inst. f. Phys. Chemie, Universität Göttingen, private communication.
[21] J. P. Monat, R. K. Hanson, and C. H. Kruger, Combust. Sci. Technol. *16*, 21 (1977).
[22] P. Roth, Deutsche Luft- und Raumfahrt, Forschungsbericht 71-62, 1971, DFVLR, Köln-Porz.
[23] W. C. Gardiner, Jr., W. G. Mallard, and J. H. Owen, J. Chem. Phys. *60*, 2290 (1974).
[24] G. L. Schott, P. W. Getzinger, and W. Seitz, Int. J. Chem. Kinet. *6*, 921 (1974).
[25] M. Louge and R. K. Hanson, private communication.
[26] D. Gutman, E. A. Hardwige, F. A. Dougherty, and R. W. Lutz, J. Chem. Phys. *47*, 4400 (1967).
[27] C. J. Jachimowski and W. M. Houghton, Combust. Flame *15*, 125 (1970).

(Eingegangen am 2. August 1984, endgültige Fassung am 1. Oktober 1984) E 5802

Kinetics of the Reactions of CH_2OH Radicals with O_2 and HO_2

Horst-Henning Grotheer*), Gottfried Riekert, Ulrich Meier, and Thomas Just

DFVLR-Institut für Physikalische Chemie der Verbrennung, Pfaffenwaldring 38, D-7000 Stuttgart 80, West-Germany

Chemical Kinetics / Mass Spectrometry / Radicals

The rate coefficient of the reaction $CH_2OH + O_2 \rightarrow HO_2 + CH_2O$ (1) has been measured by discharge flow mass spectrometry-technique under first order conditions with excess oxygen at room temperature to be $k_1 = (9.5 \pm 2.5) \cdot 10^{-12}$ cm^3 s^{-1}. Reaction (1) is followed by $CH_2OH + HO_2 \rightarrow$ products (4). The rate coefficients k_4 could be inferred from HO_2 measurements to be $6 \cdot 10^{-11}$ cm^3 s^{-1}, the uncertainty factor being 2.

Introduction

The reaction of hydroxymethyl radicals with molecular oxygen is believed to play an important role not only in the chemistry of methanol flames [1] but also in the ethylene removal within polluted atmospheres [2]. To our knowledge the work of Radford [3] is the only previous one dealing with this elementary reaction. He found the "unexpectedly large value" of $k = (2^{+2}_{-1}) \cdot 10^{-12}$ cm^3 s^{-1}, which had been verified by LMR measurements of the product HO_2 after having failed to find any LMR spectra of CH_2OH. Therefore, we attempted to study this reaction more directly by mass spectrometric measurements of the CH_2OH radical under O_2 excess conditions.

Experimental

We carried out the experiments at room temperature, pressures ranging from 0.4 to 1.2 mbar and flow velocities up to 30 ms^{-1}. Different fast flow reactors were used with diameters of approximately 4 cm, lengths 25 or 50 cm, made of teflon or quartz (HF washed or coated with halocarbon wax) with a movable inlet. In the case of the HO_2 experiments, we used a double injector, the two jets being separated by 3 cm and constructed such as to optimize mixing. All gas flow meters have been calibrated. Gas samples were taken by means of a molecular beam sampling system and analyzed by a TOF mass spectrometer.

CH_2OH Production

CH_2OH radicals were produced by the fast reaction of $CH_3OH + Cl$ which generates [4] CH_2OH in large excess over CH_3O radicals. The latter has been confirmed by our mass spectrometric experiments with deuterated methanols, i.e. CH_3OD and CD_3OH, as well as by LIF experiments [5]. In order to obtain the CH_2OH concentration at the O_2 injection point, one has to account for the following reaction sequence:

$$CH_3OH + Cl \longrightarrow CH_2OH + HCl \quad (5)$$

$$CH_2OH + Cl \longrightarrow CH_2O + HCl \quad (6)$$

$$CH_2OH + CH_2OH \longrightarrow C_2H_6O^* \xrightarrow{M} C_2H_6O_2 \quad (2a)$$

$$\longrightarrow \dot{C}HOH + CH_3OH\,. \quad (2b)$$

The products of reaction (2b) were $\dot{C}HOH$ and CH_3OH which was found by experiments with deuterated methanols.

The rate coefficients k_6 and k_{2a+b} have been measured in a separate study [6] to be $1.4 \cdot 10^{-10}$ cm^3 s^{-1} and $1.5 \cdot 10^{-11}$ cm^{-3} s^{-1}, (2b) is the minor channel. Based on this reaction sequence we roughly estimated the $[CH_2OH]_0$ values in Figs. 1 and 2. Whenever a better knowledge of $[CH_2OH]_0$ was needed it has been determined by computer simulation and/or calibration (see below). CH_3OH usually was in a 100 – 1000 fold excess over Cl.

CH_2OH measurements were carried out at ionization energies below 11 eV, thus nearly suppressing the occurrence of the 31 amu fragmentation peak of the excess methanol, which was less than 5% of the CH_2OH signal.

Results

$CH_2OH + O_2$

O_2 was added to the CH_3OH/CH_2OH-flow by a movable injector. This portion of the flow was shown to be free from Cl atoms but not entirely free from Cl_2 molecules. Continuous displacement of the O_2 injector led to CH_2OH vs. t profiles as shown in Fig. 1. Especially in the low pressure regime the resulting slopes must be corrected for viscous pressure drop and axial diffusion. This has been done according to the well known expressions [7] which led to corrections of up to 5% for the pressure drop and 15% for the diffusion in the case of lowest pressure and highest O_2 concentrations. The resulting data from various experiments are shown in Fig. 2. A least squares fit yields an

*) Present address: Brookhaven National Laboratory, Upton 11973, P.O. Box 427, USA.